KSCE Journal of Civil Engineering (2015) 19(4):917-928
DOI 10.1007/s12205-014-0741-6

Geotechnical Engineering
pISSN 1226-7988, eISSN 1976-3808
www.springer.com/12205

Three Dimensional Numerical Analysis of the Effects of Tunnelling Near Piled Structures

A. F. Zidan* and O. M. O. Ramadan**

Received December 17, 2013/Revised April 8, 2014/Accepted June 2, 2014/Published Online December 31, 2014

Abstract

The construction of tunnels in soft ground leads to ground movements. In urban areas with soft soils, these movements can affect the safety of surface structures. This paper investigates the interaction between tunnelling in soft soil and adjacent piled structure. Several three-dimensional finite element analyses are performed to study the deformation of pile caps and piles during the construction of a nearby tunnel. Comparison between free field and coupled analyses is also presented. To simulate the tunnelling process and its effects on piled structures, one symmetric half of the soil medium, the tunnel boring machine, the face pressure, the final tunnel lining, the pile caps, and the piles are modelled in several construction phases. The first part of the paper describes the adopted numerical model. Then, pile cap movements as well as pile deformation and bending moments resulting from the tunnelling process are investigated. The influence of the superstructure stiffness and its gravity load level on the tunnelling-produced response of the pile foundation is also investigated. Finally, the results of coupled analyses, which include the superstructure, are compared to those obtained using the analysis of piles alone (excluding the superstructure). This comparison helps to evaluate the later type of analysis that is typically implemented in routine designs.

Keywords: *tunnelling, soil-structure interaction, piled structure, strain-hardening, finite element, three-dimensional analysis*

1. Introduction

Construction of tunnels requires assessing their impact on existing structures particularly for tunnelling in soft grounds near pile foundation (Attewell *et al.*, 1986; Forth and Thorley, 1996; Lee *et al.*, 1994; Chen *et al.*, 1999). This may result in increasing pile deformations and altering the distribution of internal forces in piles, pile caps, and the supported superstructure (Vermeer and Bonnier, 1991; Bezuijen and Schrier, 1994; Mroueh and Shahrour, 2002; Lee and Ng, 2005; Lee *et al.*, 2007; Cheng *et al.*, 2007). Various empirical relationships between tunnelling induced ground movement and associated structure damage were introduced based on the analysis of previous case histories (Burland and Wroth, 1974; Boscardin and Cording, 1989; Burland, 1995; Mair *et al.*, 1996). The study of the effect of tunnelling on nearby pile foundation began with laboratory investigation performed by Morton and King (2011). Besides, centrifuge modelling was also used to investigate tunnelling induced ground and pile deformations (Loganathan *et al.*, 2000; Hegarden *et al.*, 1996; Jacobsz *et al.*, 2001; Ong *et al.*, 2007; Ng *et al.*, 2013) and the significant lateral and vertical forces on nearby piles was reported. Numerical investigations were also performed using two simplified stages. In the first stage, the ground movements due to tunnelling are calculated using empirical, analytical or numerical methods such as those proposed by Peck (1969), O'Reilly and New (1982), and Sagaseta (1987). In the second stage, the building response to tunnelling is determined by subjecting the building structure to the soil movements calculated in step 1. Thus, this approach does not account for the structure-tunnel interaction.

Various factors that affect the tunnelling-induced response of single piles and pile groups have been studied (Mroueh and Shahrour, 2002; Cheng *et al.*, 2007; Yang *et al.*, 2011; Yao *et al.*, 2012; Lee, 2012; Linlong *et al.*, 2012, Lee, 2013; Ng *et al.*, 2013). Numerical results showed that tunnelling induces significant internal forces in adjacent piles. The distribution of these induced internal forces depends mainly on the position of the pile tip relative to the tunnel horizontal axis as well as the distance between the pile axis and the tunnel.

Analysing the structure-foundation-soil interaction during tunnelling operation in a single, coupled analysis is cumbersome due to: (i) the high interaction between tunnelling in soft soils and adjacent, relatively-stiff structures; (ii) the problem three-dimensional nature; and (iii) the expected high non-linear behaviour of soft soils. Rigorous, realistic analysis of such conditions can

*Assistant Professor, Dept. of Civil Engineering, Faculty of Engineering, Beni-Suef University, Beni-Suef 62511, Egypt (Corresponding Author, E-mail: ahmedzidan@eng.bsu.edu.eg, ahmedzidan2008@gmail.com)
**Professor, Faculty of Engineering, Cairo University; Vice-Dean, The High Institute for Engineering at Shorouk City, Cairo 62511, Egypt (E-mail: omoramadan@yahoo.ca)

only be done using full, three-dimensional models that properly simulate the presence of existing structure, its foundation, appropriate material behaviour, and the tunnelling operation (Augarde *et al.*, 1995).

This paper evaluates the complex interaction of tunnel, soil, piles, pile caps, and superstructure elements using a three-dimensional finite element analysis model to capture the response of piled structure during tunnelling. The tunnelling process is simulated in several stages by progressive removal of elements in presence of the various structure elements (piles, pile caps, columns, beams, roofs). Besides, interface elements are employed to model the possible sliding and/or separation between piles and soil. Finally, the results of the three-dimensional coupled analysis are compared to that of a simplified analysis that simulates a free field situation (in absence of the structure). The latter type of analysis is studied in order to evaluate this type of model that is sometimes adopted in routine design. This study contributes to the already wealth literature in the subject in the following aspects: it investigates the case of installing shallow tunnels directly beneath structures that are supported on long piles extending deeper than the tunnel trough; it addresses the effects of the superstructure relative stiffness and gravity load intensity; and it examines the effect of tunnelling on the behaviour of pile caps and on piles internal forces.

2. Numerical Modelling

Numerical simulations are performed by means of the finite element program PLAXIS 3D tunnel which is a flexible tool for the analysis of three-dimensional, non-linear soil–structure interaction problems (Brinkgreve, 2000). Due to symmetry of the analysed problem, only one half of the tunnel-soil-structure system is analysed. Analysis of the tunnelling–structure interaction problem is performed in two stages. The first stage determines the initial stresses in the soil mass and is performed in drained condition prior to the tunnel construction. It is performed considering the self-weight of both the soil and the structure. In the second stage, the analysis is performed under undrained condition. The displacements are reset to zero before starting of the tunnel installation to ensure that all deformations referred to hereafter are only a result of the tunnel construction.

Several construction phases are analysed to simulate the tunnelling process. The tunnel construction is modelled by progressive removal of elements. A uniform support pressure (face pressure) is applied at the tunnel face to prevent active failure of the soil in front of the Tunnelling Boring Machine (TBM). The influence of the grout injection at the shield tail is simulated by a distributed load acting over one slice. The length of this slice is typically taken 3m in places that are far from the structure while near the structure this length is reduced to match the structure geometry. Thereafter, it is assumed that the grout has settled and dewatered enough so that no additional deformations are produced.

The various phases of the applied excavation scheme are shown schematically in Fig. 1: excavation of soil, installation of

Fig. 1. Phases Modelled in the Phased Excavation Procedure

the TBM, lowering of the water level inside the TBM, application of the tunnel face pressure, and application of contraction. The tunnel face pressure and the grout pressure (p) in this study are assumed 100 and 160 kN/m^2, respectively, at the topmost levels. The grout pressure increases linearly with depth by a rate of 10 kN/m^2 per meter. On the other hand, the face pressure increases linearly with depth by the assumed bulk density of the slurry of 13 kN/m^2 (Kasper and Meschke, 2006).

The soil volume is modelled by means of 15-node triangular prism elements. Hardening-soil model (El Sawwaf, 2007; Zidan, 2012) is adopted in this numerical study to simulate the non-linear behavior of soil. This model adopts a hyperbolic relationship between the strain, ε, and the deviatoric stress, q. In the present analysis, the initial effective stress is generated by means of the k_0 procedure. The soil strength is described by means of the effective cohesion (c'), angle of internal friction (ϕ'), angle of dilatancy (ψ), failure ratio (R), and interface reduction factor (R_{intf}). The stress strain relationship is described by the secant Young's modulus (E_{50}^{ref}), the odometer modulus E_{oed}^{ref}), Poisson's ratio (ν), and the unloading reloading modulus (E_{50ur}^{ref}). A refined mesh is adopted to minimize the effect of mesh dependency on results. Table 1 lists the numerical values adopted for these soil parameters. The unit weight of soil is assumed to be 17 kN/m^3 and 20 kN/m^3 for the dry and saturated conditions, respectively.

The stiffness properties of TBM section (plate elements): membrane "axial" rigidity, EA, and flexural rigidity, EI, are input as material properties. The plate is homogeneous and isotropic, in the sense that, everywhere in the plate, the membrane and flexural rigidity parameters (per unit length) do not change with direction. For numerical calculations, an equivalent thickness for the plate (d_{eq}) is calculated based on values of its rigidity parameters, EI and EA as (PLAXIS, 2001):

$$d_{eq} = \sqrt{12\frac{EI}{EA}} \tag{1}$$

The TBM is slightly conical; the tail radius is assumed 20 mm less than the front radius. This effect has been modelled using a total contraction of 0.40% in volume.

The behaviour of the interface elements which are applied around the tunnel to model the possible slippage between soil and tunnel is described by Coulomb's criterion. For numerical

Table 1. Soil Parameters

parameter	C' (kPa)	φ' (o)	Ψ (o)	E_{50}^{ref} (kPa)	E_{oed}^{ref} (kPa)	E_{ur}^{ref} (kPa)	ν	p^{ref} (kPa)
Value	5	25	0	2000	2000	5000	0.2	100

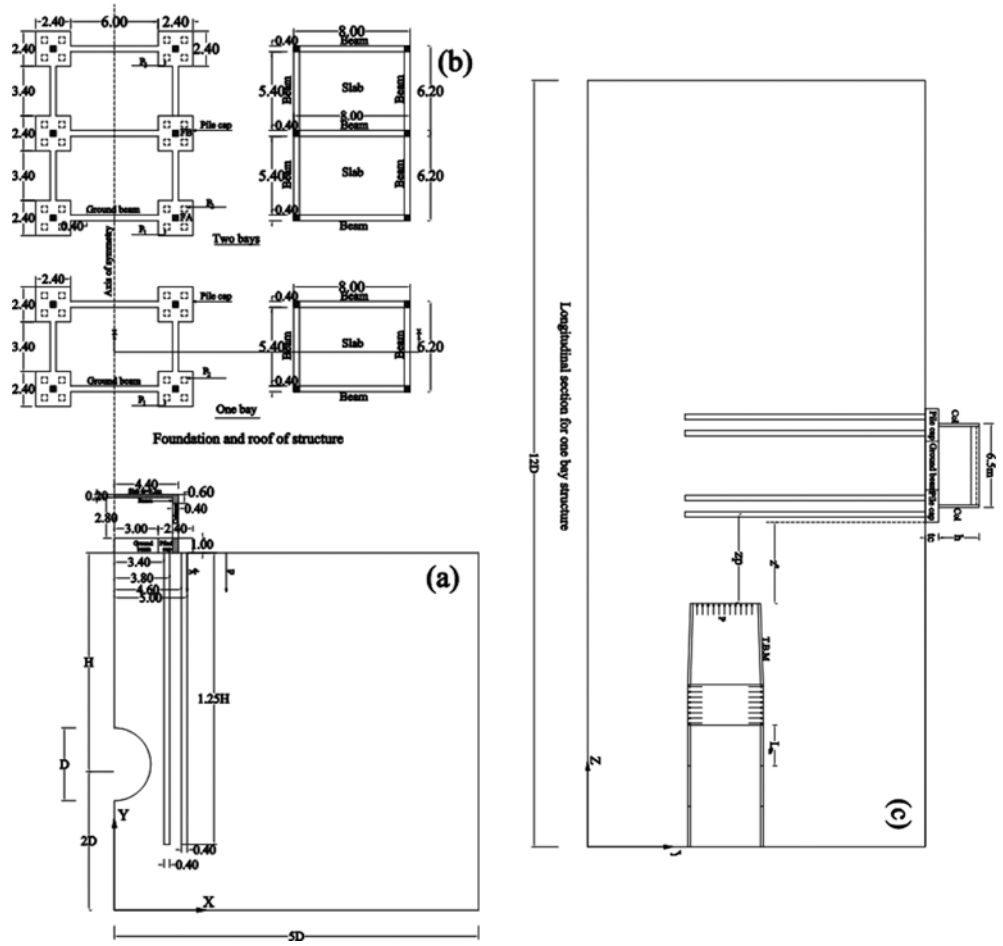

Fig. 2. Model Geometry: (a) Transverse Section Elevation, (b) Plan, (c) Longitudinal Section Elevation

applications, the soil properties' reduction factor, R_i, is taken equal to 0.7 which is appropriate for friction between clay and concrete (PLAXIS, 2001).

The structure reinforced concrete elements (square piles, pile caps, columns, beams, slabs) and the tunnel lining are modelled using 15-node volume elements with a specific weight $\gamma = 25$ kN/m^3, Young's modulus $E = 2 \times 10^7$ kN/m^2, and Poisson's ratio $\nu = 0.2$. The tunnel characteristics are given by: diameter $D = 5$ m, lining thickness $t = 0.35$ m and depth below ground surface $H = 3D$. The dimensions of the structure and the model geometry under consideration are presented in Fig. 2.

The position of structure with regard to the tunnel is defined using the following parameters:

L = length of pile
L_{lin} = tunnel face progress (distance) in each stage,
y_p = distance from bottom of pile cap to any point on the pile length.
z^* = distance from tunnel face to the front edge of pile cap,
zp = distance from tunnel face to the axis of pile under consideration

As shown in the Fig. 2, each pile cap contains four piles. For illustration and discussion of results, the three piles (P1, P2, and P3) shown in Fig. 2 are selected. The three selected piles give a good indication for the behaviour of other piles in the group. The mesh presented in Fig. 3 is used for finite element analyses. This mesh includes 8550 elements and 42970 nodes. The lateral mesh boundaries are located at a distance of 5D from the tunnel midpoint in order to minimize the impact of boundary conditions on the solution. Computations are carried out in 19 successive steps.

Figure 4 shows an example of deformed mesh during the progress of tunnelling for the case of superstructure with two bays. Besides, Table 2 describes the various types of analyses used in this paper.

3. Verification

As an overall verification of the developed model, its results are compared to those described by Peck (1969) and O'Reilly & New (1982) for the Green field site (M_1). Peck (1969) stated that the transversal settlement trough can be described by a Gaussian error function and this mathematical description has been widely accepted since then. Following this approach, the vertical settle-

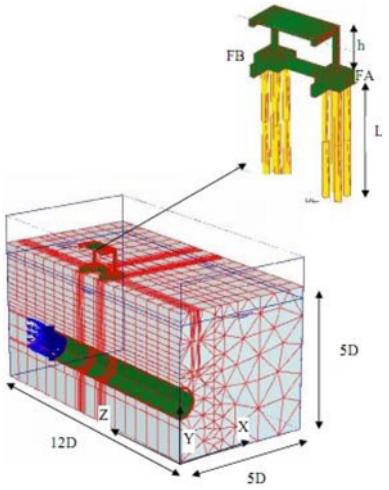

Fig. 3. Example of 3-D Coupled Analysis in Case of One-Bay Superstructure

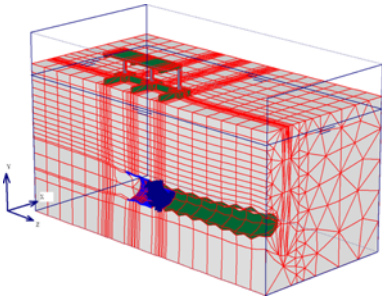

Fig. 4. Example of the Model Deformation during Tunnel Construction in Case of Two-Bay Superstructure (Displacement is Scaled to 50 Times)

Table 2. Analyzed Models

Model Label	Model description	Number of bays in structure*	Vertical load level (structure height)
M_1	Greenfield site.	Not applicable	Not applicable
M_2	Free piles (without structure).	Not applicable	5 levels
M_3	Tunnelling under piled structure.	One bay	5 levels
M_4	Tunnelling under piled structure.	Two bays	5 levels
M_5	Tunnelling under piled structure.	One bay	10 levels

*Along tunnel longitudinal axis.

ment in the transverse direction is given by:

$$S_{v(x)} = S_{v,\max} e^{-\frac{x^2}{2i_x^2}} \quad (2)$$

Besides, O'Reilly and New approximated the surface horizontal displacement by:

$$S_{hx}(x) = -\frac{x\, S_v(x)}{z_0} \quad (3)$$

where, i_x = The trough width parameter,

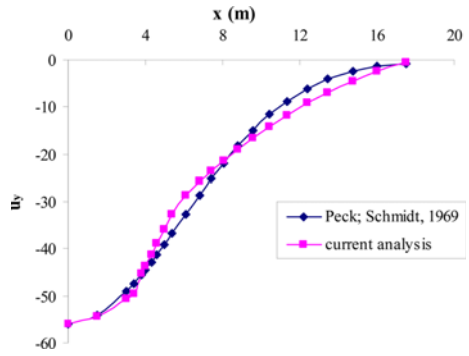

Fig. 5. Surface Vertical Displacement Obtained by 3-D Finite Element Compared to those of Peck (1969)

$S_{v(x)}$ = The vertical settlement at distance x from the tunnel centre,

$S_{v,\max}$ = The maximum settlement measured above the tunnel axis,

z_0 = Depth from ground surface to tunnel axis.

The results showed that the maximum ground settlement $S_{\max}$ is equal to 55 mm, which is about 1.1% of the tunnel diameter D. The trough width parameter (i_x) which is defined as the distance from the tunnel centreline to the point of inflection is about 5.9 m which is equal to 0.4z where z is the distance to the tunnel centre. This value agrees with the values proposed by O'Reilly and New. Figs. 5 and 6 compare the steady state surface vertical and horizontal displacements at z/D = 0.5, respectively, obtained by the 3-D finite element model to those published by Peck (1969) and O'Reilly and New (1982). These figures show good agreement between the results especially in the proximity of the superstructure. Using this observed maximum settlement for the Green field condition, the volume loss resulting from tunnelling process depending on Gaussian function (Peck, 1969) as given by Eq. (2) is about 4%.

$$S_{\max} = \frac{Vs}{i\sqrt{2\pi}} \quad (4)$$

where, i is the horizontal distance from the tunnel axis to the

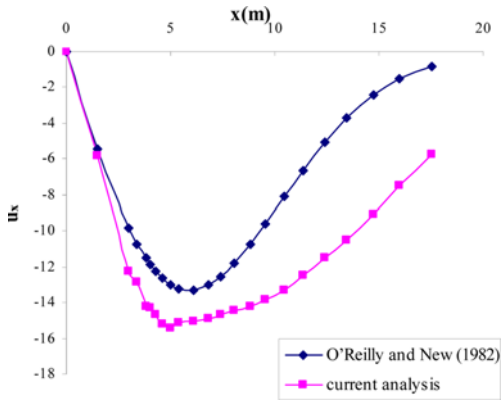

Fig. 6. Surface Horizontal Displacement Obtained by 3-D Finite Element Compared to those of O'Reilly and New (1982)

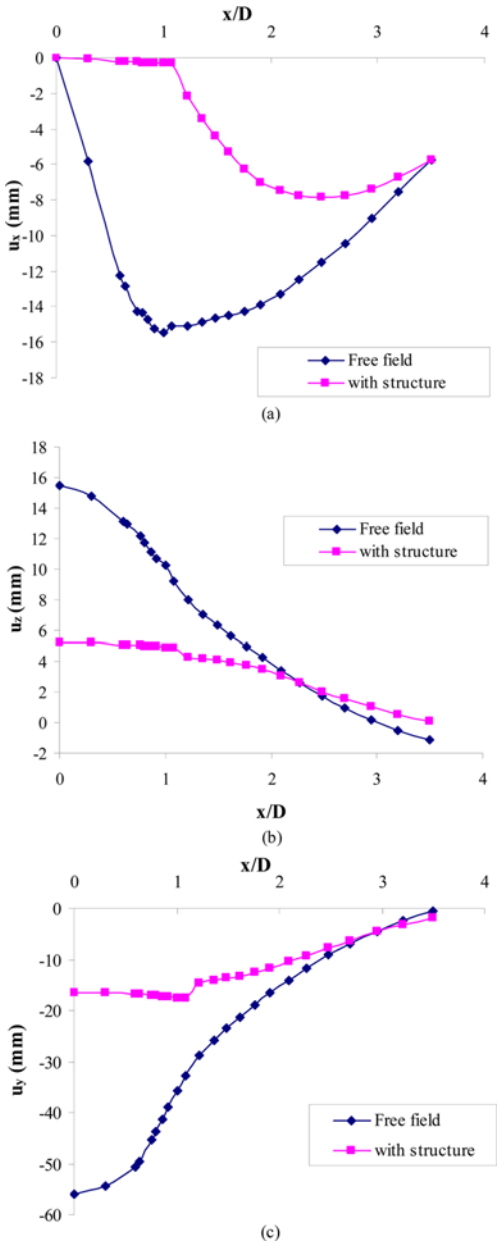

Fig. 7. Ground Surface Displacements for Free Field (M_1) and Coupled (M_3) Analyses: (a) x-Direction, (b) z-Direction, (c) y-Direction

point of inflection of the settlement trough, and *Vs* is the settlement volume per unit length.

4. Effect of Tunnelling on Soil Deformation

Figure 7 presents the results obtained from models M_1 and M_3 for the displacement of ground surface in directions of all coordinates (u_x, u_y, and u_z) induced by the tunnel construction under one bay structure. It is obvious from this figure that the presence of structure affects the ground surface deformations especially beneath the ground beam and pile caps. Figure 7(a) shows that the structure presence significantly reduces (almost eliminates) the horizontal (transverse) displacement in its vicinity. As we move away from the structure, the horizontal displacements from both the coupled analysis (M_3) and the free field analysis (M_1) approach each other and become equal at *x*-distances larger than *3D*. Besides, Fig. 7(b) shows that, compared to the free field case, the presence of the superstructure considerably reduces the longitudinal displacement (in *z* direction) under the structure foundation, but this displacement becomes larger than the value corresponding to free field analysis for $x \geq 2D$. For the case of coupled analysis, Fig. 7(c) shows that the settlement (u_y) is almost flat in the vicinity of the structure, has a sudden decrease thereafter, and becomes close to that of the free field case at moderate distances away of the structure ($x \geq 2.5D$). Figure 7(c) also shows that, within the superstructure neighbourhood, the settlement (u_y) predicted from the analysis which includes the superstructure (model M_3) is much less than that calculated from the Green field case (model M_1). The decrease in soil settlement in M_3 relative to M_1 indicates that the piles, which extend deeper than the tunnel trough in the present analysis, actually support the soil above the tunnel and increase the arching mechanism. This behaviour is further verified by the increase in pile axial forces due to tunnelling as presented below.

5. Effect of Tunnelling on Pile Caps

Figure 8 shows the displacement of the structure foundations at front (FA) and rear (FB) pile caps with the tunnel construction progress for the two cases of coupled (M_3) and free field (M_1) analyses. Significant effects of structure presence on the transverse displacement (u_x) are evident from Fig. 8(a). The lateral displacement (u_x) under structure foundation is very small compared to the free field analysis at the location of FA and FB; this is partially due to assuming the tunnel axis to be at the centre of the building in this study. Besides, Fig. 8(b) shows that the longitudinal displacement of structure foundations (u_z) increases as the tunnel face approaches the pile cap. Therefore, the maximum displacement occurs when the tunnel face crosses the pile cap. As the structure stiffness is accounted for in the coupled analysis, the results show that no relative displacement takes place in *z* direction between FA and FB.

The vertical settlement of pile caps (FA and FB) is presented in Fig. 8(c) which shows that the settlement of foundation increases during tunnelling. For the coupled case, the settlement reaches about 75% and 40% of its maximum value for FA and FB, respectively, when the tunnel face crosses the edge of the first pile cap FA ($z^* = 0$). The maximum settlement observed under both pile caps in free field analysis is more than double that calculated from the coupled analysis because the long piles strengthened the soil mass above the tunnel and thus increased the arching action. The maximum differential settlement between FA and FB is about 40% of the maximum overall settlement for both the coupled and free field analyses. Thus, the maximum differential settlement between pile caps for the coupled analysis is less than 50% of the corresponding value for the free field analysis.

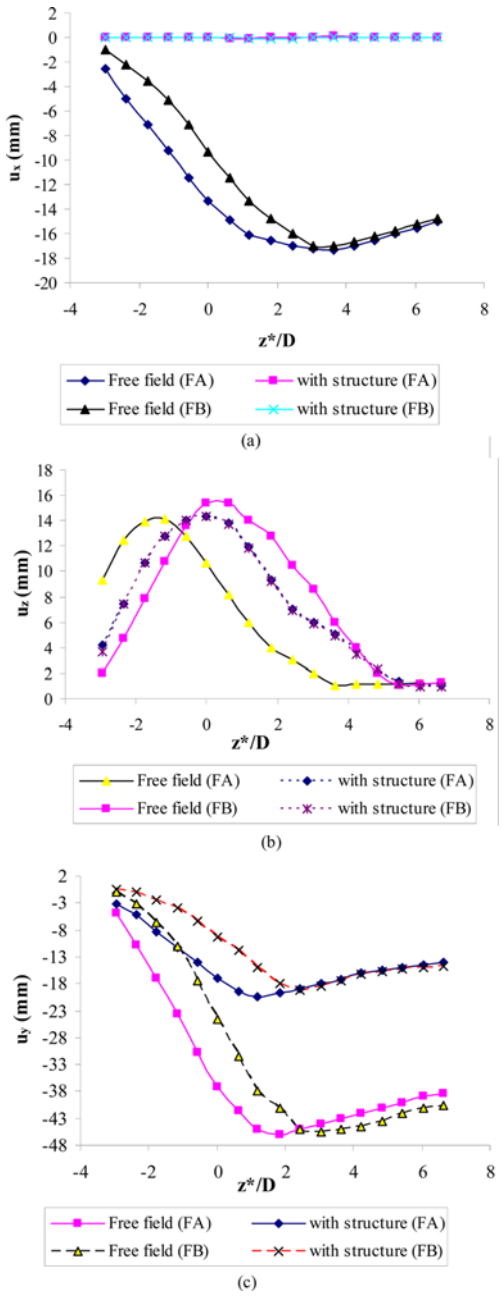

Fig. 8. Pile Cap Displacements during Tunnelling for Front (FA) and Rear (FB) Caps from Coupled (M_3) as well as Free Field (M_1) Analyses: (a) x-Direction, (b) z-Direction, (c) y-Direction

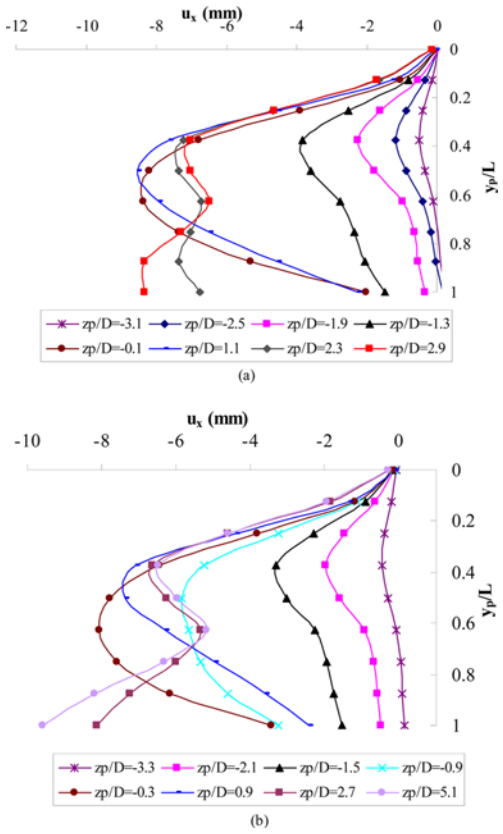

Fig. 9. Pile Deformation in x-Direction during Tunnelling for One Bay Structure (M_3): (a) P1, (b) P2

6. Effect of Tunnelling on Piles

6.1 General Pile Behaviour

It is well known that the progress of tunnel construction induces deformation in piles located near the tunnelling zone. The group of curves presented in Fig. 9 shows the deflected shapes of piles P1 and P2 in the "transverse" XY plane (u_x) for the case of one bay structure and coupled analysis (model M_3). These figures show that, when the tunnel face is approaching the pile, the transverse deflection u_x increases with the progress of tunnelling and its maximum value occurs in the middle third of the pile. After the tunnel face moves across the pile, the transverse deflection in the pile middle third decreases with the progress of tunnel construction and its maximum value shifts position to the pile tip. The piles deflect in double- or triple-curvature while tunnel construction is progressing towards the structure. Furthermore, as the construction operation goes on past the structure, the piles curvature continues to increase. Therefore, higher internal forces develop in the piles after the tunnelling operation passes the structure location.

Figure 10 shows the distribution of the pile deflection along the tunnel longitudinal axis (i.e. u_z) for piles P1 and P2 (model M_3). It indicates that as the tunnel face progresses towards the structure, u_z increases and has its highest value at pile heads. However, after tunnelling operation passes the pile locations, values of u_z at pile heads decrease while the values at pile tips increase as the tunnel face progresses away of the structure. The deflections at pile tips are higher than those at pile heads. Comparing Figs. 9 and 10, it is seen that while the pile deflections along the tunnel longitudinal axis (u_z) are higher than the transverse ones (u_x), the curvatures and consequently the bending moments and shear forces are higher in the transverse direction (i.e. in the XY plane).

6.2 Pile Internal Forces

Due to size limitation, pile internal forces are briefly discussed.

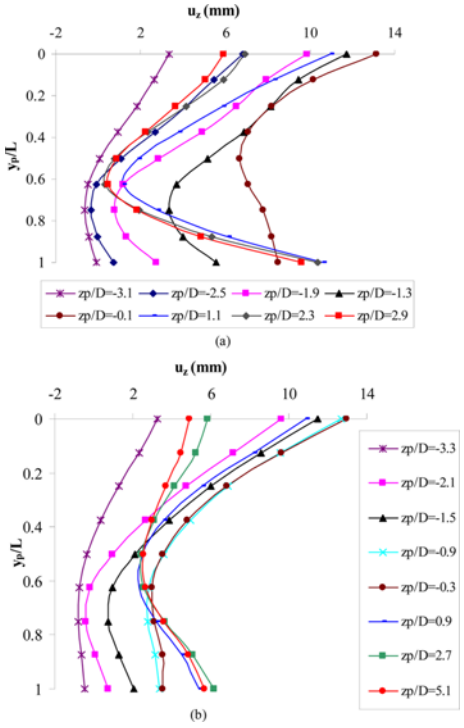

Fig. 10. Pile Deformation in z-Direction during Tunnelling for One Bay Structure (M_3): (a) P1, (b) P2

Effect of tunnelling on pile axial loads is discussed followed by tunnelling effect on pile bending moment.

6.2.1 Pile Axial Loads

The stresses obtained from the finite element analysis are integrated to calculate the pile axial loads. The axial load in piles P1 and P2 due to the 5-storey structure load alone (prior to start of tunnelling) was 464 kN and 556 kN, respectively. During tunnelling (for model M_3), the pile axial loads in P1 and P2 increased monotonically and reached 558 kN and 683 kN, respectively. This indicates that the soil mass above the tunnel is partially supported by the piles and explains why the settlement (u_y) predicted from the analysis which includes the superstructure (model M_3) is much less than that calculated from the Green field case (model M_1) as depicted in Fig. 7(c). Note that the support provided by the piles to the soil mass above the tunnel must not be considered a general rule as it is specifically attributed to the present analysis with long piles extending deeper than the tunnel trough. Despite the advantage of reducing soil settlement, this behaviour increases the risk on the piled structure as a result of increasing pile axial loads by up to 23%.

6.2.2 Pile Bending Moment

Bending moment in each pile is calculated as the product of its flexural rigidity EI_p and its curvature, u''. The curvature is estimated by numerically differentiating the corresponding lateral displacement (deflection) u for the considered plane: XY or YZ. The distribution of pile bending moment (M_z) resulting from bending in the transverse plane (plane XY) as well as its variations with tunnelling progress was qualitatively and quantitatively similar for piles P1 and P2. The peak bending moment values increased monotonically with the progress of tunnelling operation and attained their maximum values ($|M_z| \leq 20$ kNm) at end of tunnelling. However, the distribution of pile bending moment (M_x) resulting from its bending in the YZ plane as well as its variations with tunnelling progress for pile P1 was different from those of pile P2. Besides, the peak bending moment values attained their maxima during tunnelling and not at end of tunnelling. The maximum value of bending moment in pile P1 was slightly less than its bending in transverse plane (for P1: $|M_x| \leq 16$ kNm) while that of pile P2 was much less (for P2: $|M_x| \leq 8$ kNm). An

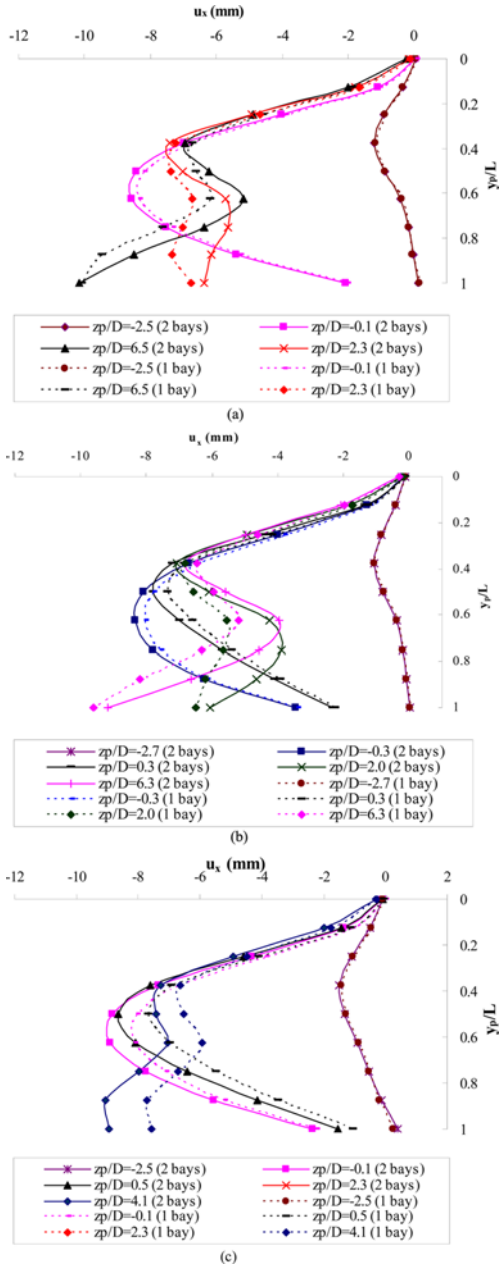

Fig. 11. Effect of Structure Continuity on Pile Deformation (u_x) during Tunnelling: (a) P1, (b) P2, (c) P3

important observation is that these bending moments changed locations along the pile length during tunnelling and almost covered the full pile length.

The results presented above show that tunnelling near piled structures, with piles extending below excavated tunnel, may threaten pile structural safety in two ways: (1) by increasing pile axial loads (as soil above tunnel hangs on the piles); and (2) by producing significant bending moments in piles. The bending moments due to tunnelling are significant for two reasons: (1) they extend over the full pile length while piles are not typically reinforced over their full length in practice; and (2) the obtained bending moments correspond to eccentricities $e = M/P$ of up to 10% of pile size, which are higher than the typical 5% minimum design eccentricity ratio.

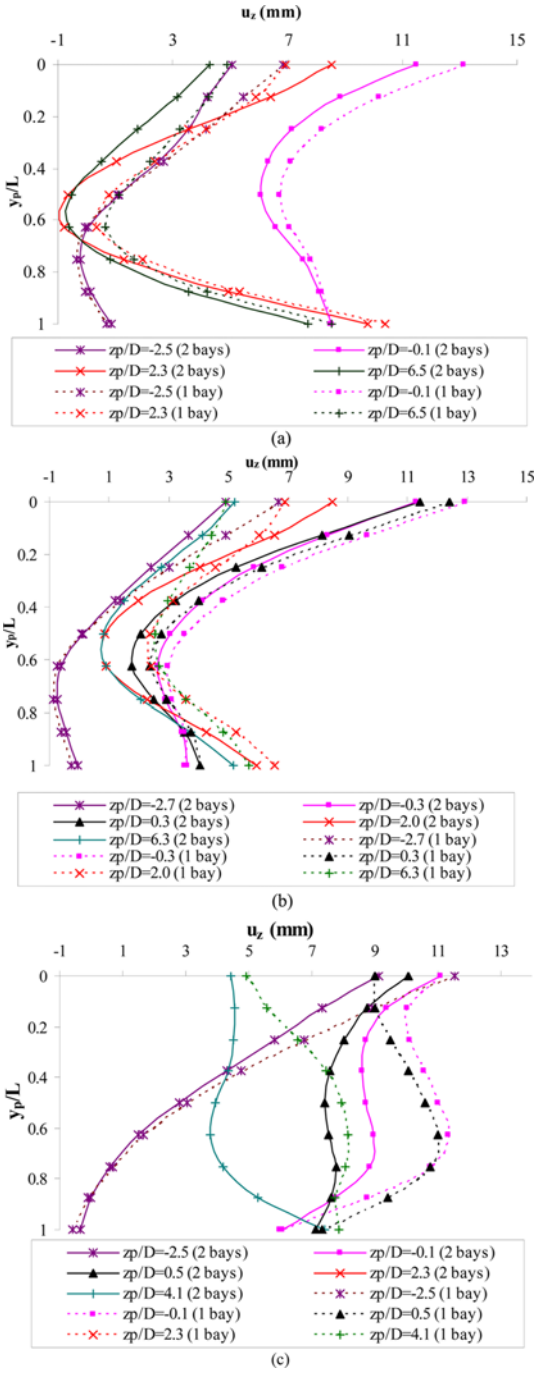

Fig. 12. Effect of Structure Continuity on Pile Deformation (u_z) during Tunnelling: (a) P1, (b) P2, (c) P3.

7. Effects of Superstructure Characteristics

7.1 Effect of Superstructure Continuity on Piles

Figure 11 shows the effect of structure continuity- along the tunnel longitudinal axis- on the deformation in x direction for piles (P1, P2& P3). These results are obtained by models M_3 and M_4. No significant effects of the building continuity are observed on the values of u_x and M_z for the three piles when the tunnel face is progressing towards the piles. After the tunnel face crosses the piles' location and continues to progress, the distributions of u_x and M_z are marginally affected by superstructure continuity but their peak values are practically unchanged. In particular, the lateral deformation at piles' tip is slightly affected by the continuity of structure.

The effect of the structure continuity on piles' deformation in z direction is depicted in Fig. 12. It is noted that the structure continuity decreases the piles' displacement in z direction and this is more pronounced for the rear pile (P3). Compared to the case of one-bay superstructure, the maximum reduction in u_z due

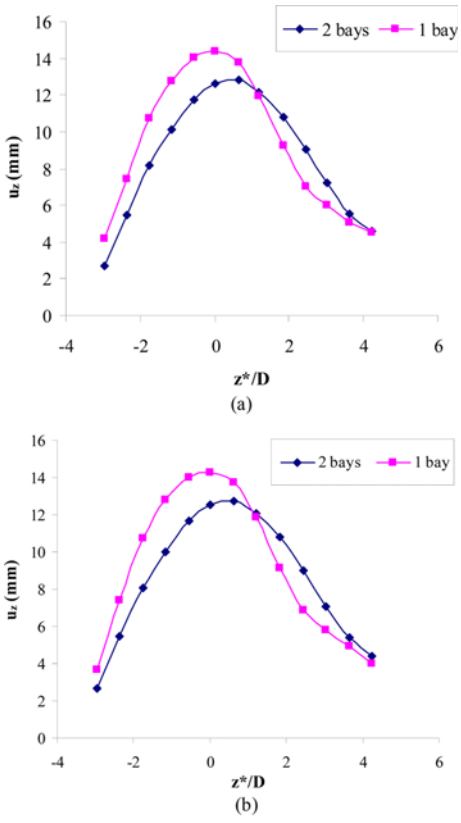

Fig. 13. Effect of Structure Continuity on Pile Cap Movement in z-Direction for Cases of One-Bay (M_3) and Two-Bay (M_4) Structure: (a) Front Cap FA, (b) Rear Cap FB

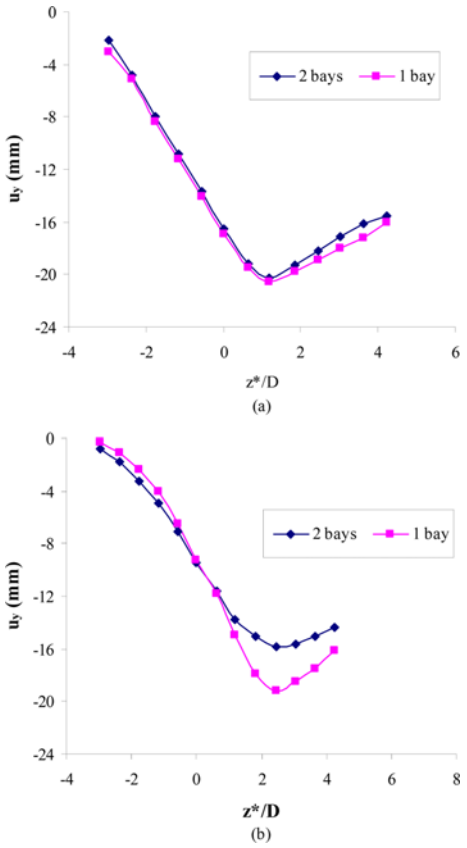

Fig. 14. Effect of Structure Continuity on Pile Cap Movement in y-Direction (Settlement) for Cases of One-Bay (M_3) and Two-Bay (M_4) Structure: (a) Front Cap FA, (b) Rear Cap FB

to superstructure continuity is 13%, 12%, and 48% for piles P1, P2, and P3, respectively.

7.2 Effect of Superstructure Continuity on Pile Caps

To explore the influence of structure continuity on pile cap movements, Figs. 13 and 14 show the effect of building continuity on the movements of front and rear pile caps for two conditions of the superstructure system along the tunnel longitudinal axis: one-bay and two-bay. Note that the two-bay structure is stiffer and has higher degree of statical indeterminacy than the one-bay one. As a result, pile cap movements of the two-bay structure are clearly less than those of the one-bay structure. Besides, Fig. 13 indicates that the reduction in the peak value of the pile cap transverse movement u_x due to superstructure continuity is about 12% for pile caps FA and FB. Moreover, Fig. 14 shows that, compared to the one-bay structure, the maximum settlement of the two-bay structure is reduced by 2% and 20% for pile caps FA and FB, respectively.

To explore the influence of structure continuity on its pile foundation, Fig. 15 shows variation in the differential settlement between front and rear caps with tunnelling progress obtained by models M_3 and M_4. This figure shows that the maximum differential settlement occurred when the tunnel face crossed the front cap (FA). Also, the minimum differential settlement is observed when the tunnel face moves away from the rear footing (FB) and attains the steady state settlement. Moreover, it is seen that the differential settlement between pile caps slightly decreased for the case of two-bay structure.

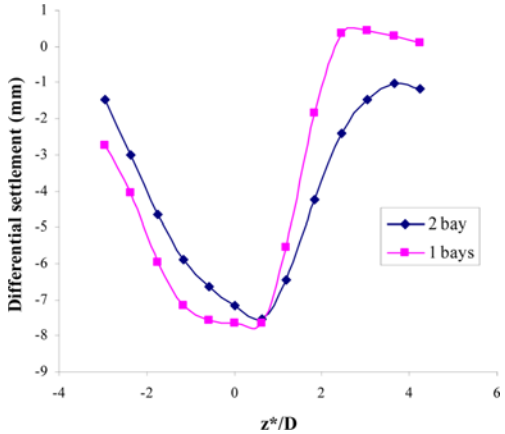

Fig. 15. Differential Settlement between Front (FA) and Rear (FB) Caps with Tunnel Construction for Cases of One-Bay (M_3) and Two-Bay (M_4) Structure

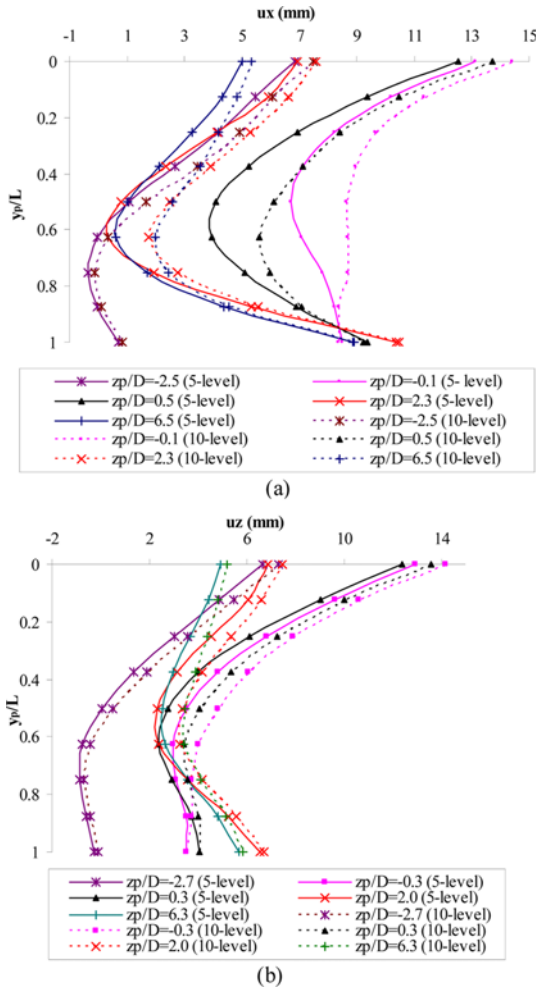

Fig. 16. Effect of Superstructure Vertical Load Level on Pile Deformation (u_z) during Tunnelling: (a) P1, (b) P2

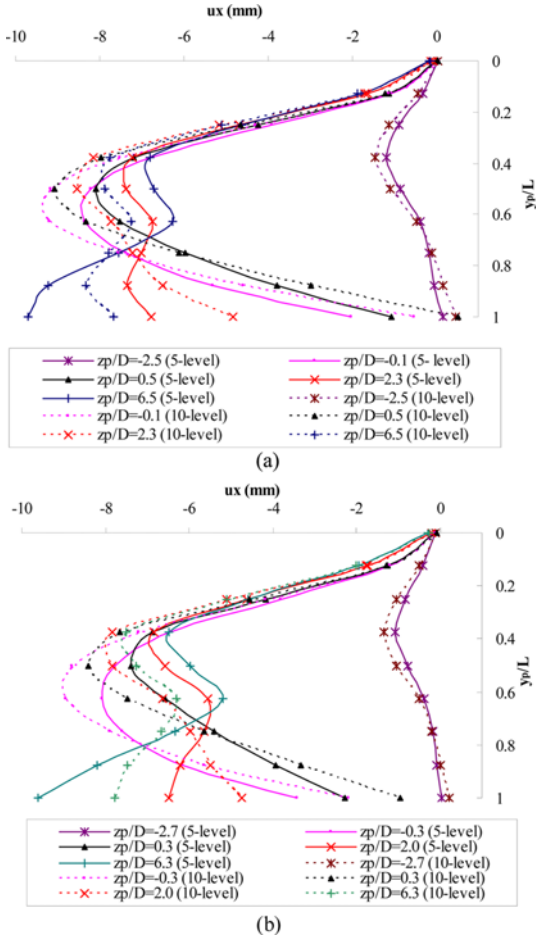

Fig. 17. Effect of Superstructure Vertical Load Level on Pile Deformation (u_x) during Tunnelling: (a) P1, (b) P2

7.3 Superstructure Vertical Load Level

To investigate the effect of the superstructure vertical loads on the piles deformation during tunnelling the one-bay superstructure models M3 and M5 are adopted. Two values for the superstructure loads are considered to simulate buildings with 5 stories and 10 stories, respectively. Figure 16 shows that the deformation parallel to the tunnel longitudinal axes (u_z) of piles P1 and P2 considerably increases when the number of floors is increased from 5 to 10; more so for pile P1. Besides, Fig. 17, which presents similar data but for (u_x), points out that the piles transverse deformation in their lower half is significantly affected by the increase in superstructure vertical loads.

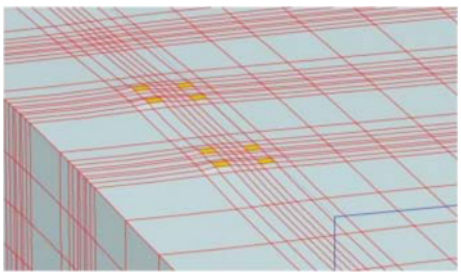

Fig. 18. Modelling of Tunnelling-Free Piles Interaction

7.4 Tunnelling-Structure Interaction

In the analyses presented so far, the structure elements (e.g. pile caps, columns, beams, and slabs) were included. In this section, piles are loaded with the same loads as in the coupled analysis but are assumed to be free from constraints at their heads as depicted in the three dimensional model of tunnelling-free piles interaction model shown in Fig. 18. In order to evaluate such type of simplified analysis, we compare the results of coupled analysis (M_3) to that of free field, without superstructure, analysis (M_2).

Figure 19 illustrates the effect of the modelling assumption (including/excluding the superstructure elements and stiffness) on the piles' transverse deformation (u_x) while Fig. 20 presents the same data for the piles' longitudinal deformation (u_z) for P1 and P2. It is observed from Fig. 19 that neglecting the influence of superstructure interaction results in large differences in estimating the transverse deformation of pile heads. While the superstructure stiffness in the analysed example almost fully constrains the pile heads, significant displacements of pile heads are observed when the superstructure is not included in the analysis model. Besides, neglecting the influence of the super-

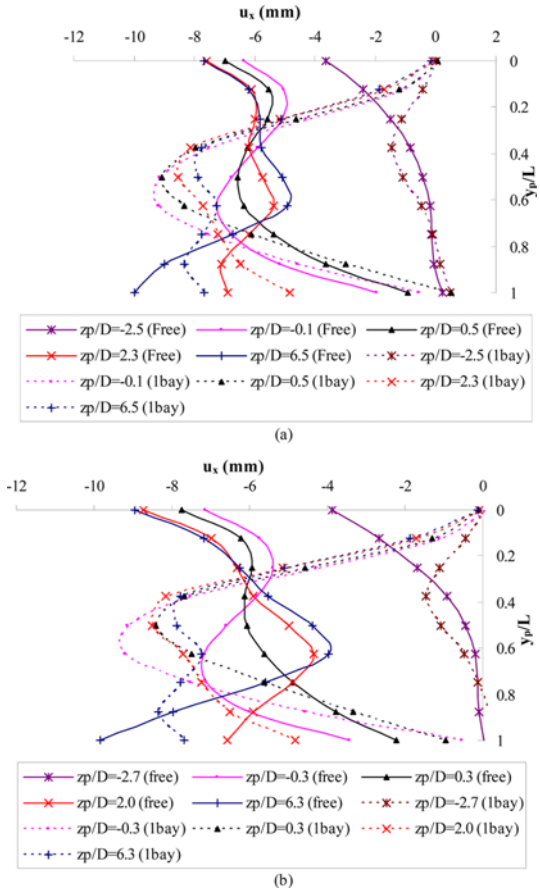

Fig. 19. Influence of Super-Structure Interaction on Piles' Transverse Deformation (u_x) during Tunnelling for One Bay Structure: (a) P1, (b) P2

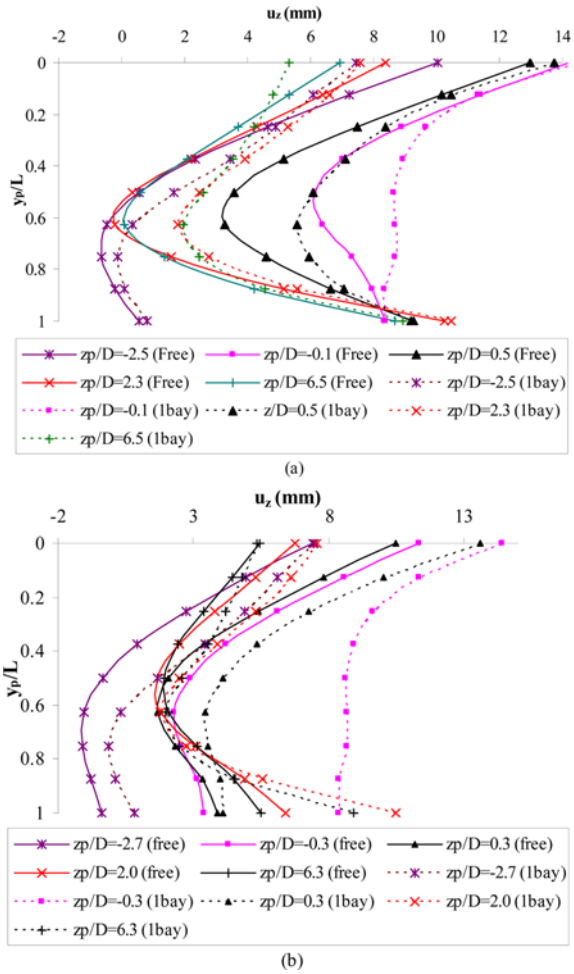

Fig. 20. Influence of Super-Structure Interaction on Piles' Longitudinal Deformation (u_z) during Tunnelling for One Bay Structure: (a) P1, (b) P2

structure also alters the pile deflection everywhere along its length. When combined together, the differences resulting from neglecting the superstructure interaction significantly reduce the curvature of piles and, consequently, underestimate pile internal forces. Finally, Fig. 20 shows that the effect of superstructure interaction on the longitudinal deformation of piles (u_z) is less-pronounced than its effect on pile transverse deformation although still significant.

8. Conclusions

This paper investigates the influence of tunnelling in soft soils beneath a pile-supported structure for various interaction scenarios. Based on the obtained numerical results and subject to the case study geometry and assumptions, the following conclusions are drawn.

The maximum response values for piles as well as pile caps do not necessary occur at end of tunnelling but some critical responses attain their peak values during tunnelling particularly just after the tunnel face passes by the structure element under consideration. Thus, structural safety checks must consider the full tunnelling process and cannot be based on final situation.

Compared to the complete analysis which includes the stiffness of the superstructure, the often made assumption of free piles (ignoring the interaction with the superstructure) is found to be unjustified. Numerical results showed that the free-pile analysis underestimates the flexural response of piles by more than 20%.

Tunnelling beneath piled structures produces considerable differential settlements between pile caps- about 40% of maximum overall settlement. Besides, significant bending moments are produced over the full pile length due to tunnelling. This poses risks on piles that are reinforced over its top portion only.

Tunnelling near piled structures, with piles extending below excavated tunnel as in the present study, increases pile axial loads as soil above tunnel is partially supported by the piles. This reduces soil settlement but increases the risk on the piled structure as a result of increasing pile axial loads by up to 23% for the present case study.

The effect of the superstructure vertical load level on piles' deformation during tunnelling is found to be secondary particularly when realizing that the increased superstructure load shall accompanied with a proportional increase in pile size and/or number.

References

Attewell, P. B., Yeates, J., and Selby A. R. (1986). *Soil movements induced by tunnelling and their effects on pipelines and structures*, Blackie, Glasgow & London.

Augarde, C. E., Burd, H. J., and Houlsby, G. T. (1995). "A three-dimensional finite element model of tunnelling." *Proc. 4th Symp. on Numerical models in Geomechanics-NUMOG V, Davos, Swizerland*, Balkama, Rotterdam, pp. 457-462

Bezuijen, A. and Schrier Van der, J. (1994). "The influence of a bored tunnel on pile foundations." *Proceedings of the International Conference Centrifuge 94*, pp. 681-685.

Boscardin, M. D. and Cording, E. G. (1989). "Building response to excavation induced settlement." *ASCE Journal of Geotechnical Engineering*, Vol. 115, No. 1, pp. 1-21, DOI: 10.1061/(ASCE)0733-9410(1989)115:1(1).

Burland, J. B. (1995). "Assessment of risk damage to buildings due to tunnelling and excavation." *Proc. 1st International Conference on Earthquake and Geotechnical Engineering*, IS-Tokyo.

Burland, J. B. and Wroth, C. P. (1974). "Settlements on buildings and associated damage." *Proceedings of Conference on Settlement of structures*, BTS, Cambridge, pp. 611-654.

Brinkgreve, R. B. J. (2000). *Plaxis 3D tunnel program*, Vermeer, P.A.

Chen, L. T., Poulos, H. G., and Loganathan, N. (1999). "Pile responses caused by tunnelling." *ASCE Journal of Geotechnical and Geoenvironmental Engineering*, Vol. 125, No. 3, pp. 207-215, DOI:10.1061/(ASCE)1090-0241(1999)125:3(207).

Cheng, C. Y., Dasari, G. R., Chow, Y. K., and Leung, C. F. (2007). "Finite element analysis of tunnel–soil–pile interaction using displacement controlled model." *Tunnelling and Underground Space Technology*, Vol. 22, No. 4, pp. 450-466, DOI: 10.1016/j.tust.2006.08.002.

El Sawwaf, M. (2007). "Behavior of strip footing on geogrid reinforced

sand over a soft clay slope." *Geotextiles and Geomembranes*, Vol. 25, No.1, pp. 50-60, DOI: 10.1016/j.geotexmem.2006.06.001.

Forth, R. A. and Thorley, C. B. B. (1996). "Hong Kong island line predictions and performance." *Proc. Int. Geotechnical Aspect of Underground Construction in soft Ground*, Balkema, Rotterdam, pp. 677-682.

Hergarden, H. J. A. M., Van der Poel, T. J., and Van der Schrier, J. S. (1996). "Ground movements due to tunneling: Influence on pile foundations." *Proc. Int. Symposium on Geotechnical Aspects of Underground Construction in Soft Ground*, Balkema, London, pp. 519-524.

Jacobsz, S. W., Standing, J. R., Mair, R. J., Soga, K., Hagiwara, T., and Sugiyama, T. (2001). "The effects of tunneling near single driven piles in dry sand." *Proc. of Asian Regional Conference on Geotechnical Aspects of Underground Construction in Soft Ground*, Tongji University Press, Shanghai, pp. 29-35.

Kasper, T. and Meschke, Gu. (2006). "On the inuence of face pressure, grouting pressure and TBM design in soft ground tunnelling." *Tunnelling and Underground Space Technology*, Vol. 21, No. 2, pp. 160-171, DOI: 10.1016/j.tust.2005.06.006.

Lee, C. G. (2012). "Three-dimensional numerical analyses of the response of a single pile and pile groups to tunnelling in weak weathered rock." *Tunnelling and Underground Space Technology*, Vol. 32, pp. 132-142, DOI: 10.1016/j.tust.2012.06.005.

Lee, C. J. (2013). "Numerical analysis of pile response to open face tunnelling in stiff clay." *Computers and Geotechnics*, Vol. 51, pp. 116-127, DOI: 10.1016/j.compgeo.2013.02.007.

Lee, G. T. K. and Ng, C. W. W. (2005). "Effects of advancing open face tunnelling on an existing loaded pile." *Journal of Geotechnical and Geoenvironmental Engineering*, ASCE, Vol. 131, No. 2, pp. 193-201, DOI: 10.1061/(ASCE)1090-0241(2005)131:2(193).

Lee, R. G., Turner, A. J., and Whitworth, L. J. (1994). "Deformations caused by tunnelling beneath a piled structure." *Proc. the XIII International Conference on Soil Mechanics and Foundation Engineering,* University Press, London, pp. 873-878.

Lee, C. J., Jun, S. H., Yoo, N. J., and Kim, G. W. (2007). "The effects of tunnelling on an adjacent single pile." *Underground Space – The 4th Dimension of Metropolises*.

Linlong, M., Maosong, H., and Richard, J. F. (2012). "Tunnelling effects on lateral behaviour of pile rafts in layered soil." *Tunnelling and Underground Space Technology*, Vol. 28, pp. 192-201, DOI: 10.1016/j.tust.2011.10.010.

Loganathan, N., Poulos, H. J., and Stewart, D. P. (2000). "Centrifuge model testing of tunnelling-induced ground and pile deformations." *Geotechnique*, Vol. 50, No. 3, pp. 283-294, DOI: 10.1680/geot.2000.50.3.283.

Mair, R. J., Taylor, R. N., and Burland, J. B. (1996). "Prediction of ground movements and assessment of risk of building damage due to bored tunnelling." *Proc., Geotechnical Aspect of Underground Construction in soft Ground*, Balkema, Rotterdam, pp. 713-718.

Morton, J. D. and King, K. H. (2011). "Effects of Tunnelling on the bearing capacity and settlement of piled foundations." *Proc. Tunnelling 79*, IMM, London, 1979, pp. 57-68.

Mroueh, H. and Shahrour, I. (2002). "Three-dimensional finite element analysis of the interaction between tunnelling and pile foundation." *Int. J. Numer. Anal. Meth. Geomech.*, Vol. 26, No. 3, pp. 217-230, DOI: 10.1002/nag.194.

Ng, C. W. W., Lu, H., and Peng, S. Y. (2013). "Three-dimensional centrifuge modelling of the effects of twin tunnelling on an existing pile." *Tunnelling and Underground Space Technology*, Vol. 35, pp. 189-199, DOI: 10.1016/j.tust.2012.07.008.

Ong, C. W., Leung, C. F., and Chow, Y. K. (2007). "Experimental study of tunnel-soil-pile interaction." *Proc. Underground Singapore,* National University of Singapore, Singapore, pp. 256-263.

O'Reilly, M. P. and New, B. M. (1982). "Settlements above tunnels in United Kingdom their magnitude and prediction." *Proc. of Tunnelling'82,* IMM, London, pp. 173-181.

Peck, R. B. (1969). "Deep excavation and tunnelling in soft ground." *Proc. 7th International Conference on Soil Mechanics and Foundations Engineering,* State-of-Art, Mexico City, pp. 225-290.

PLAXIS (2001). *PLAXIS 3D tunnel validation and verification manual*, PLAXIS BV & Delft University, Delft, The Netherlands.

Sagaseta, C. (1987). "Evaluation of surface movements above tunnels - A new approach." *Colloque International ENPC Interactions Sols Structures,* Paris, pp. 445-452.

Vermeer, P. A. and Bonnier, P. G. (1991). "Pile settlements due to tunnelling." *Proc. 10th European Conference on Soil Mechanics and Foundation Engineering,* Florence, pp. 869-872.

Yao, A., Yang, X., and Dong, L. (2012). "Numerical analysis of the influence of isolation piles in metro tunnel construction of adjacent buildings." *Procedia Earth and Planetary Science*, Vol. 5, pp. 150-154, DOI: 10.1016/j.proeps.2012.01.026.

Yang, M., Sun, Q., Li, W.-C., and Ma, K. (2011). "Three-dimensional finite element analysis on effects of tunnel construction on nearby pile foundation." *J. Cent. South Univ. Technol,* Vol. 18, pp. 909-916, DOI: 10.1007/s11771-011-0780-9.

Zidan, A. F. (2012). "Numerical study of behaviour of circular footing on geogrid-reinforced sand under static and dynamic loading." *Geotechnical and Geological Engineering*, Vol. 30, No. 2, pp. 499-510, DOI: 10.1007/s10706-011-9483-0.